INSTITUTE OF PHYSICS PUBLISHING JOURNAL OF OPTICS B: QUANTUM AND SEMICLASSICAL OPTICS

J. Opt. B: Quantum Semiclass. Opt. **6** (2004) S404–S409 PII: S1464-4266(04)74051-3

Optical vortices near sub-wavelength structures

Hugo F Schouten[1], **Taco D Visser**[1] **and Daan Lenstra**[1,2]

[1] Department of Physics and Astronomy, Free University, De Boelelaan 1081, 1081 HV Amsterdam, The Netherlands
[2] COBRA Research Institute, Technische Universiteit Eindhoven, The Netherlands

E-mail: tvisser@nat.vu.nl

Received 22 December 2003, accepted for publication 3 March 2004
Published 4 May 2004
Online at stacks.iop.org/JOptB/6/S404
DOI: 10.1088/1464-4266/6/5/031

Abstract
In this paper the phase singularities of the electromagnetic field near a sub-wavelength slit are studied. These phase singularities, such as optical vortices, are found in regular patterns, which can be created or annihilated under the conservation of certain topological quantities, when a parameter such as the slit width is changed. The connection between the phase singularities and the light transmission though the slit is considered.

Keywords: singular optics, phase singularities, optical vortices, diffraction, electromagnetic fields, slits

(Some figures in this article are in colour only in the electronic version)

1. Introduction

A monochromatic wavefield is characterized by its local amplitude and phase. At points where the amplitude vanishes, the phase is indeterminate. Such a *phase singularity* or *vortex* can be found in many different physical systems. The first mention of *optical vortices* seems to date back to the 1950s when Braunbek and Laukien theoretically studied the diffraction of a plane wave by a perfectly conducting, infinitely thin half-plane [1, 2]. They predicted phase singularities of both a single component of the magnetic field, and the time-averaged Poynting vector field. Some 15 years later, Boivin and Wolf [3] noted that the Airy rings in a focal plane also correspond to phase singularities of the Poynting vector. In the early 1970s Landstorfer *et al* [4] calculated and measured vortices of the Poynting vector field in the near zone of antennas. In all these studies it was found that different phase singularities can coexist at a distance that is much smaller than the wavelength. The systematic study of such *topological defects* of wavefields began with a paper by Nye and Berry [5]. Nowadays several reviews of the subject are available [6–8]. In this paper we discuss some recent developments of the burgeoning field of *singular optics*.

2. Phase singularities in scalar and electromagnetic fields

We consider a complex monochromatic scalar field ψ, and write it as (suppressing the time dependence $\exp(-\mathrm{i}\omega t)$)

$$\psi(\mathbf{r}) = \rho(\mathbf{r})\mathrm{e}^{\mathrm{i}\phi(\mathbf{r})}. \tag{1}$$

A *phase singularity* is defined as a point $\mathbf{r}$ where the amplitude $\rho(\mathbf{r})$ is zero and hence the phase $\phi(\mathbf{r})$ is undefined. The condition $\psi(\mathbf{r}) = 0$ is equivalent to

$$\mathrm{Re}(\rho(\mathbf{r})) = 0, \tag{2}$$

$$\mathrm{Im}(\rho(\mathbf{r})) = 0. \tag{3}$$

These two conditions imply that phase singularities can typically be found as lines in three-dimensional space, whereas in two dimensions, they are typically separated points. The phase around a phase singularity possesses a vortex-like structure (see figure 1(a)), and increases or decreases as one moves around the singularity.

In our analysis, we study configurations and electromagnetic fields, which are invariant along the y-direction. Furthermore, we assume that the field is TE polarized. In that case the only non-zero component of the electric field is the y-component, $\hat{E}_y$. Such a field component, however, in general

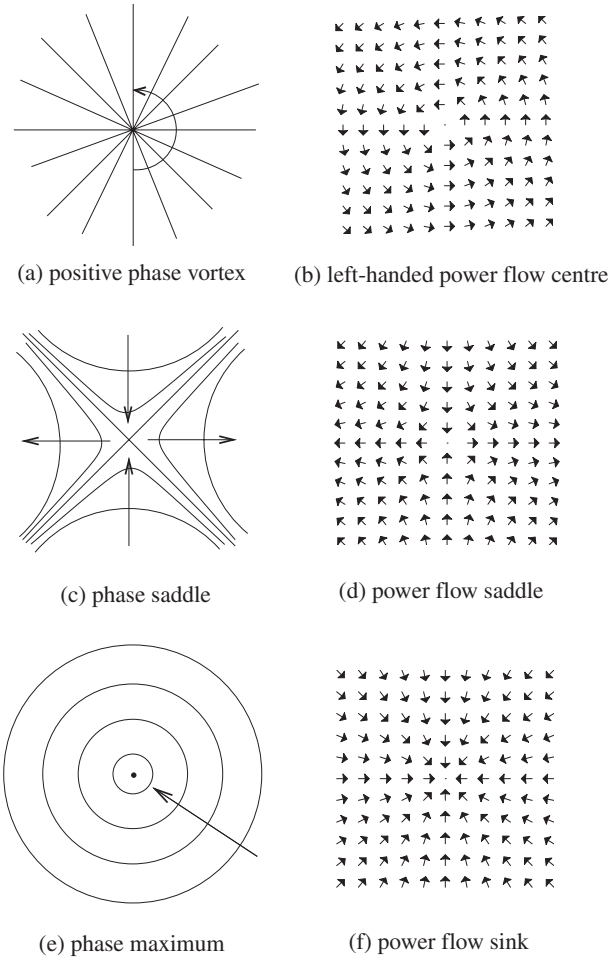

(a) positive phase vortex (b) left-handed power flow centre

(c) phase saddle (d) power flow saddle

(e) phase maximum (f) power flow sink

Figure 1. Illustrating the relation between phase singularities (a), stationary points of the phase ((c), (e)), and the corresponding singularities of the power flow ((b), (d), (f)). The arrows in the left-hand column indicate the direction of increasing phase ϕ_E.

depends on the coordinates x and z, with an amplitude and a phase that can be expressed as

$$\hat{E}_y(x,z) = |\hat{E}_y(x,z)|\mathrm{e}^{\mathrm{i}\phi_E(x,z)}. \tag{4}$$

Note that the time dependence $\exp(-\mathrm{i}\omega t)$ is again suppressed. Such a field configuration is suitable for analysing, as in section 3 below, the problem of propagation of a TE polarized field through a slit oriented parallel to the y-axis.

The electromagnetic field considered here has an associated time-averaged Poynting vector field whose only non-zero components are S_x and S_z. These components are only dependent on the coordinates x and z, so they can be expressed as

$$\mathbf{S}(x,z) = (S_x(x,z), 0, S_z(x,z)) = \tfrac{1}{2}\,\mathrm{Re}\{\hat{\mathbf{E}}(x,z)\times\hat{\mathbf{H}}^*(x,z)\}, \tag{5}$$

where $\hat{\mathbf{E}}$ and $\hat{\mathbf{H}}$ are the amplitudes of the complex monochromatic electromagnetic field. Note that this time-averaged Poynting vector can be formally considered as a two-dimensional real-valued vector field.

It is interesting to relate the singular features of the complex electric field component $\hat{E}_y(x,z)$ to those that will subsequently appear in the associated two-dimensional time-averaged real-valued Poynting vector field $\mathbf{S}(x,z)$. To this end, a 'phase' must be defined for this latter field. This is done via the pair of relations

$$\begin{aligned} \sin\phi_S(x,z) &\equiv \frac{S_z(x,z)}{|\mathbf{S}(x,z)|}, \\ \cos\phi_S(x,z) &\equiv \frac{S_x(x,z)}{|\mathbf{S}(x,z)|}, \end{aligned} \tag{6}$$

where $|\mathbf{S}|$ is the modulus of $\mathbf{S}$. The reason for this definition of ϕ_S is that it has mathematically exactly the same structure as the phase of a complex scalar field. Analogous to the case for complex scalar fields, phase singularities of the Poynting vector are defined as points where the phase is undefined, and consequently its modulus is zero.

For a field which is TE polarized, i.e. the only non-zero component of the electric field is $\hat{E}_y$, it can be readily shown using equation (5) and Maxwell's equations that

$$\mathbf{S}(x,z) = -\frac{1}{2\omega\mu_0}\,\mathrm{Im}\{\hat{E}_y\nabla\hat{E}_y^*\}. \tag{7}$$

On substituting equation (4) into (7), one finds that the Poynting vector may be expressed in the form

$$\mathbf{S}(x,z) = \frac{1}{2\omega\mu_0}|\hat{E}_y(x,z)|^2\nabla\phi_E(x,z). \tag{8}$$

For a field which is TM polarized, a similar equation holds, where the time-averaged Poynting vector is expressed in terms of the amplitude and the gradient of the phase of $\hat{H}_y$.

Equation (8) suggests that the singular points of $\mathbf{S}$ may generally be divided into two categories: those which are related to the *singular points* of the phase of $\hat{E}_y$ (where $|\hat{E}_y(x,z)| = 0$) and those which are related to the *stationary points* of the phase of $\hat{E}_y$ (for which $\nabla\phi_E(x,z) = 0$). Because these topological features of $\hat{E}_y$ are directly related to the singular points of $\mathbf{S}$, we will briefly review some properties of the singular and stationary points of $\hat{E}_y$ and their relation to the singular points of $\mathbf{S}$.

The singular points of $\hat{E}_y$ correspond to vortices (also referred to as centres) of the power flow $\mathbf{S}$, around which the power flow circulates (see figure 1(b)). A centre is referred to as right-handed (left-handed) if it is anticlockwise seen in the direction of the positive (negative) y-axis. Such a vortex clearly has $\nabla\cdot\mathbf{S} = 0$, meaning that there is no energy absorption, and therefore a centre can occur in free space. It is to be noted that in all the figures in this paper the y-axis points into the page; a left-handed or right-handed centre therefore corresponds to a positive or negative phase vortex, respectively.

At the stationary points of $\hat{E}_y$, the phase ϕ_E is well defined but its gradient vanishes. These stationary points include both minima and maxima as well as saddles, to be referred to as phase saddles (figure 1(c)). Phase saddles of $\hat{E}_y$ correspond to saddle points of the power flow, as illustrated in figure 1(d). A phase maximum (figure 1(e)) of $\hat{E}_y$ corresponds to a sink of power flow (figure 1 (f)), and a phase minimum corresponds to a source of power flow; it is to be noted that for sinks and sources $\nabla\cdot\mathbf{S} \neq 0$, and hence they cannot occur in free space. A more exotic example of a stationary point is a double phase

saddle, which is like a normal phase saddle, but has three directions in which the phase increases and three directions in which the phase decreases. A double phase saddle of $\hat{E}_y$ corresponds to a so-called monkey saddle [9] of the power flow. Other, more exotic phase singularities are possible, but not typical. They are usually unstable, i.e., under a small perturbation of the field they decay into the simple phase singularities described above.

Both phase singularities and stationary points are topological features of the complex field $\hat{E}_y$, and several conserved quantities can be associated with each of them. The first of these is the so-called *topological charge* s_E of the field, defined as the integral of $\nabla\phi_E$ around a closed loop enclosing the feature, i.e.,

$$s_E \equiv \frac{1}{2\pi}\oint_C \nabla\phi_E \cdot \mathrm{d}\mathbf{r}, \tag{9}$$

where C is a closed anticlockwise path of winding number 1. It can be shown that the topological charge of a given phase singularity takes on a unique positive or negative integer value, independent of the choice of the enclosing path C. Likewise, the topological charge of a phase saddle, maximum or minimum is always zero.

Another quantity of interest is the *topological index* t_E, which is defined as the topological charge of the phase singularities of the vector field $\nabla\phi_E$. It can be shown that for both a positive and a negative vortex $t_E = +1$, whereas for a phase saddle $t_E = -1$. The topological index of a phase maximum or minimum is $t_E = +1$, whereas for a double phase saddle $t_E = -2$.

A topological charge s_S and index t_S can also be associated with the phase ϕ_S of the power flow. It follows directly from equation (8) that the topological *charge* of $\mathbf{S}$ for a given feature is equal to the topological *index* of $\hat{E}_y$. Therefore, the topological charge of a vortex of the power flow $s_S = +1$, regardless of whether it is a positive or negative vortex of $\hat{E}_y$. Similarly, the topological charge of a saddle point of the power flow $s_S = -1$, the topological charge of a source or sink $s_S = +1$, and the topological charge of a monkey saddle $s_S = -2$. Also, a topological index may be defined for the singularities of the power flow, but this is not necessary for our interests and will not be considered here.

Both topological charge and index are quantities which are conserved under smooth variations of the configuration parameters, and as such they can only appear or disappear via creation and annihilation of multiple stationary and/or singular points. The commonest process involves the creation (annihilation) of a positive vortex ($s_E = +1$, $t_E = +1$), a negative vortex ($s_E = -1$, $t_E = +1$), and two phase saddles ($s_E = 0$, $t_E = -1$ for each). This event may also be described in terms of the creation/annihilation of phase singularities of the field of power flow; see figure 2. In this figure, some possible reactions are shown. Other, more complex, events are also possible, but are not typical.

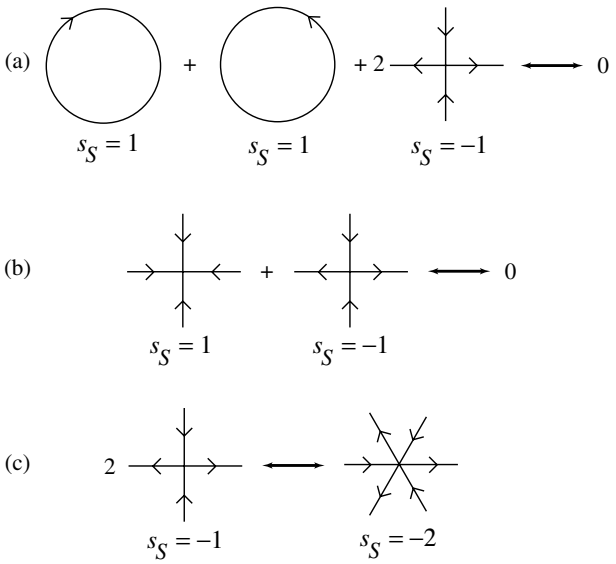

Figure 2. Illustrating some of the possible reactions between phase singularities of the time-averaged Poynting vector field: (a) the annihilation (creation) of two vortices of opposite direction and two saddle points; (b) the annihilation (creation) of a saddle point and a sink; (c) the creation (decay) of a monkey saddle out of two saddle points.

3. Optical vortices near a sub-wavelength slit

A rigorous scattering approach [10] was used to calculate the field in the vicinity of an infinitely long slit in a metal plate. This method takes into account the finite conductivity and finite thickness of the plate. The illuminating field is taken to be monochromatic with time dependence $\exp(-\mathrm{i}\omega t)$. For the electric field this scattering problem reduces to solving the following integral equation [10]:

$$\hat{\mathbf{E}} = \hat{\mathbf{E}}^{(\mathrm{inc})} - \mathrm{i}\omega\Delta\varepsilon \int_{\mathrm{slit}} \mathsf{G}\cdot\hat{\mathbf{E}}\,\mathrm{d}^2 r, \tag{10}$$

where $\Delta\varepsilon = \varepsilon_0 - \varepsilon_{\mathrm{plate}}$ is the difference in permittivity between the slit (vacuum) and the plate, and G is the electric Green's tensor pertaining to the plate without the slit. The incident field $\hat{\mathbf{E}}^{(\mathrm{inc})}$ is the field that would occur in the absence of the slit in the plate. Here it is taken to be a plane wave propagating perpendicular to the plate with the electric field polarized along the slit. It is to be noted that the incident field also consists of a reflected part and a part that is transmitted by the plate. The second term on the right-hand side of (10) is the scattered field due to the presence of the slit. For points within the slit, (10) is a Fredholm equation of the second kind for $\hat{\mathbf{E}}$, which is solved numerically by the collocation method with piecewise-constant basis functions [11].

In figure 3 a typical example of the behaviour of the time-averaged Poynting vector is shown. It can be seen that the field exhibits several phase singularities. There are two optical vortices (a and b) *within* the plate, which correspond to a 'funnel-like' power flow into the slit. In addition, five other phase singularities are visible just below the slit (c, d, e, f, and g; three saddle points and two vortices). If the time-averaged Poynting vector is plotted in the same region for a somewhat wider slit (see figure 4), a similar pattern can be seen. However, the power flow through the slit has increased, and instead of three, only two saddle points are present (e and f). The other saddle point does still exist, but has moved below the plotted region. This can be seen in figure 6, where the location of the phase singularities is shown on a large scale. It is seen that

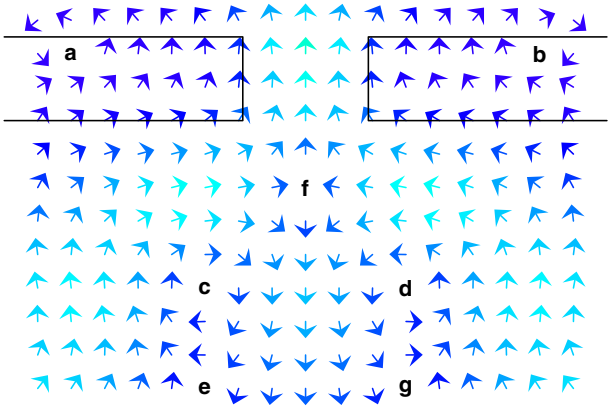

Figure 3. The behaviour of the time-averaged Poynting vector near a 150 nm wide slit in a 100 nm thick silver plate. The incident light (coming from below) has a wavelength $\lambda = 500$ nm. The left-handed (a and d) and right-handed optical vortices (b and c) each have a topological charge of +1, whereas the topological charge of the saddle points (e, f, and g) is -1. The transmission coefficient $T = 0.51$. The shading indicates the modulus of the Poynting vector (see the legend of figure 5).

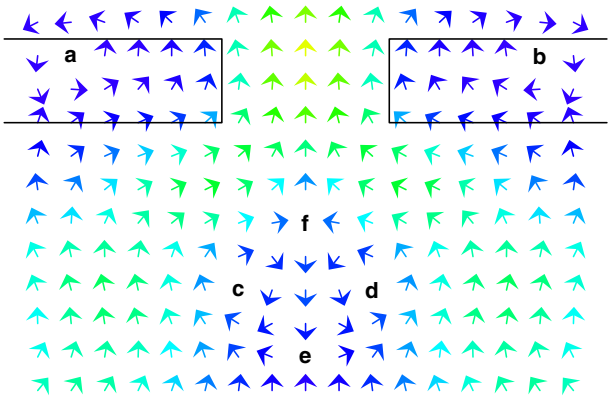

Figure 4. The behaviour of the time-averaged Poynting vector near a 200 nm wide slit in a 100 nm thick silver plate. The incident light (coming from below) has a wavelength $\lambda = 500$ nm. The transmission coefficient $T = 1.11$. The shading indicates the modulus of the Poynting vector (see the legend of figure 5).

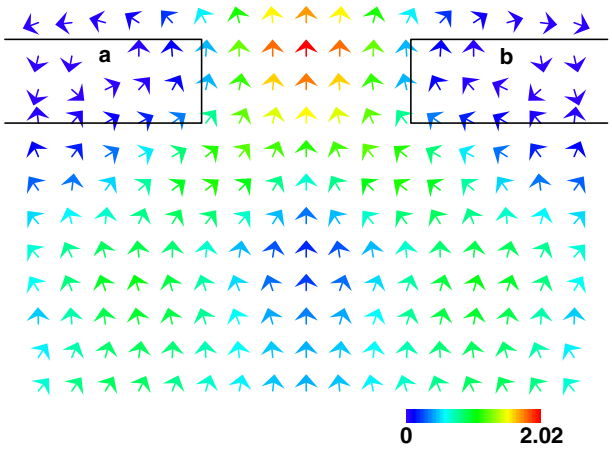

Figure 5. The behaviour of the time-averaged Poynting vector near a 250 nm wide slit in a 100 nm thick silver plate. The incident light (coming from below) has a wavelength $\lambda = 500$ nm. The transmission coefficient $T = 1.33$. The shading indicates the modulus of the Poynting vector (see the legend).

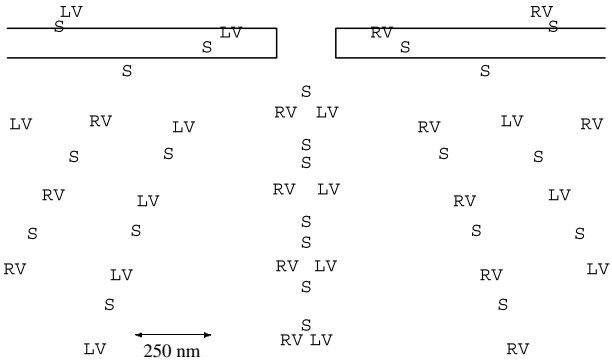

Figure 6. Location of phase singularities in the field of power flow for the same configuration as in figure 4, i.e. for a slit width of $w = 0.4\lambda = 200$ nm. The left- and right-handed optical vortices are denoted by LV and RV, respectively; S denotes a saddle point. Notice the larger scale as compared to figure 4.

they are arranged in an array-like pattern. It is to be noted that only parts of the phase singularities are shown—the pattern is continuous in a periodic way to the left and right, and also downwards. It was found that at least 5000 phase singularities are present for this particular example.

In figure 5 the time-averaged Poynting vector is shown in the same region as in figures 3 and 4, but now for a configuration with an even wider slit. The four phase singularities below the plate in figure 4 are not present any longer; they have annihilated each other (topological charge being conserved in the process). In fact, the other phase singularities present on the symmetry axis (see figure 6) are also annihilated. This coincides with an enhanced power flow through the slit.

The annihilation of the phase singularities occurs because of the changes in the guided modes inside the slit. More specifically, at $w \approx 0.4\lambda$ the first guided mode changes from evanescent to propagating [12]. Due to this change, the incident field can more efficiently couple to the guided mode, which results in a qualitatively different power flow. Similar annihilations, but now of different arrays of phase singularities in the power flow [13], occur when other guided modes change from evanescent to propagating.

In figure 7, the time-averaged Poynting vector is plotted around a 100 nm wide slit in a silicon plate. In the case of a silver plate (e.g., figure 3), two vortices are visible, which correspond to a funnel-like power flow into the slit. In contrast, the power flow near a slit in a silicon plate exhibits two vortices and two saddle points located inside the slit, coinciding with a power flow into the plate rather than into the slit. Notice the different handedness of the vortices: vortex a in figure 3 is left handed, whereas vortex b in figure 7 is right handed. In figure 8 a detail of figure 7 is shown. There it can be observed that in this region a sink and a saddle point are present. Due to conservation of energy, a sink is only possible inside a lossy material. If the width of the slit is decreased, the sink and the saddle point annihilate each other, a process in which the topological charge is again conserved.

In figure 9 the field of power flow is shown in the dashed region depicted in figure 7, but now for a slightly wider slit. In this figure, a monkey saddle singularity (e) is present. The

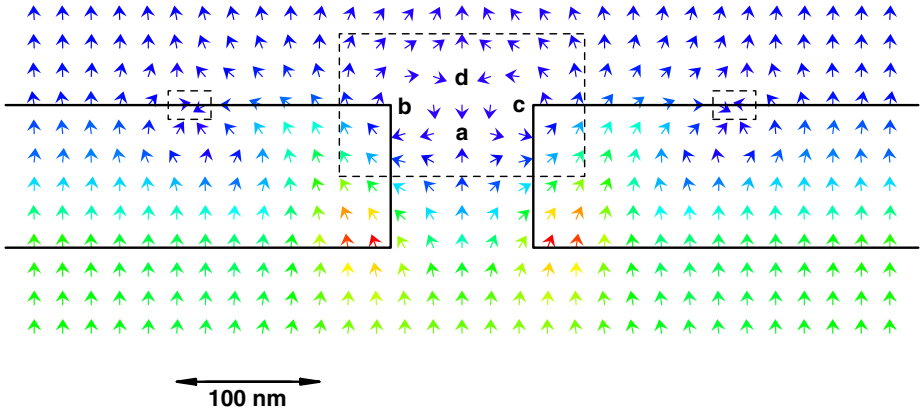

Figure 7. The behaviour of the time-averaged Poynting vector near a 100 nm wide slit in a 100 nm thick silicon plate. The incident light (coming from below) has a wavelength $\lambda = 500$ nm. Two vortices (b and c) and two saddle points (a and d) are present in the middle region. In the smaller dashed regions on the right and the left a saddle point and a sink are present (see figure 8). The dashed box in the middle denotes the region depicted in figure 9 for a different slit width.

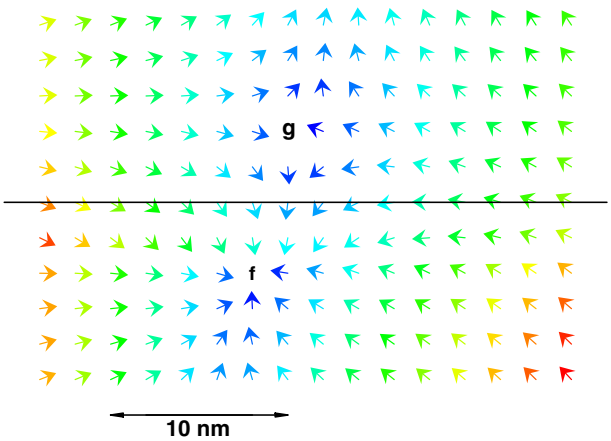

Figure 8. Detail (from the right-hand side) of figure 7. A sink (f) and a saddle point (g) are present.

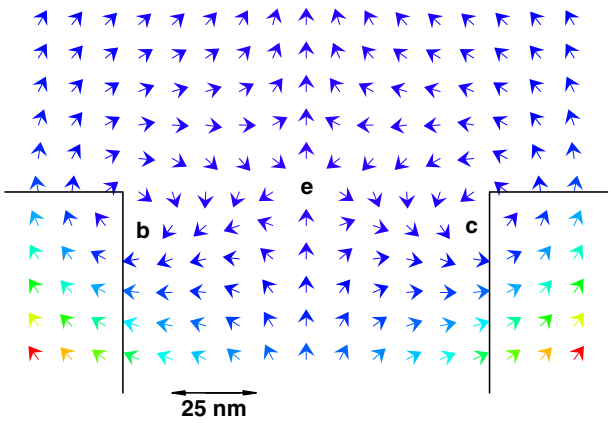

Figure 9. The time-averaged Poynting vector near a 109.5 nm wide slit in a 100 nm thick silicon plate. A monkey saddle (e) with topological charge -2 can be seen.

monkey saddle is unstable, as it exists for one value of the slit width only; for a larger width it decays into two saddle points [14]. With the aid of symmetry considerations, one can show that the singularity in figure 9 is indeed a monkey saddle, and not two closely spaced saddle points.

4. Discussion

We have shown that the field of power flow near a sub-wavelength slit possesses numerous phase singularities. The phase singularities are present in a regular array-like form. Furthermore, these arrays of phase singularities can annihilate, under conservation of topological charge, if the slit width is changed. This is related to effects such as *enhanced* transmission [12] and *frustrated* transmission [14]. Enhanced (frustrated) transmission is the phenomenon where an aperture transmits more (less) light than one expects on the basis of geometrical optics considerations [15, 16].

We note that the configurations under consideration consist of linear materials. Clearly, the occurrence of phase singularities does not require a non-linear response.

For TM polarized light, surface plasmons may be generated [17]. Their influence on the light transmission process will be discussed elsewhere.

Further study of the sub-wavelength features of optical fields may lead to increased resolution in microscopy, or an ability to 'write' information on an optical disk with a higher density than is currently possible.

Acknowledgment

This research was supported by the Dutch Technology Foundation STW.

References

[1] Braunbek W and Laukien G 1952 *Optik* **9** 174–9
[2] Born M and Wolf E 1999 *Principles of Optics* 7th (expanded) edn (Cambridge: Cambridge University Press) pp 652–7
[3] Boivin A, Dow J and Wolf E 1967 *J. Opt. Soc. Am.* **57** 1171–5
[4] Landstorfer F, Meinke H and Niedermair G 1972 *Nachr. tech. Z.* **25** 537–76
[5] Nye J F and Berry M V 1974 *Proc. R. Soc.* A **336** 165–90
[6] Nye J F 1999 *Natural Focusing and the Fine Structure of Light* (Bristol: Institute of Physics Publishing)
[7] Soskin M S and Vasnetsov M V 2001 *Progress in Optics* vol 42, ed E Wolf (Amsterdam: Elsevier) pp 219–76
[8] Allen L, Barnett S M and Padgett M J 2003 *Optical Angular Momentum* (Bristol: Institute of Physics Publishing)

[9] Hsiung C C 1981 *A First Course in Differential Geometry* (New York: Wiley) p 266
[10] Visser T D, Blok H and Lenstra D 1999 *IEEE J. Quantum Electron.* **35** 240–9
[11] Atkinson K E 1976 *A Survey of Numerical Methods of Fredholm Equations of the Second Kind* (Philadelphia, PA: SIAM) chapter 2
[12] Schouten H F, Visser T D, Lenstra D and Blok H 2003 *Phys. Rev.* E **67** 036608
[13] Schouten H F, Visser T D, Gbur G, Lenstra D and Blok H 2003 *Opt. Express* **11** 371–80
[14] Schouten H F, Visser T D, Gbur G, Lenstra D and Blok H 2003 *J. Opt. A: Pure Appl. Opt.* **6** S277–80
[15] Ebbesen T W, Lezec H J, Ghaemi H F, Thio T and Wolff P A 1998 *Nature* **391** 667–9
[16] Gacía-Vidal F J, Lezec H J, Ebbesen T W and Martín-Moreno L 2003 *Phys. Rev. Lett.* **90** 213901
[17] Raether H 1988 *Surface Plasmons on Smooth and Rough Surfaces and on Gratings* (Berlin: Springer)